*Acta Orthop. Belg.*, 2018, **84**, 307-315

*ORIGINAL STUDY*

# Morphological abnormalities of the femur in the dysplastic hip. Relation between femur en acetabulum

Peter Mahieu, Takehito Hananouchi, Nobuyuki Watanabe, Peter Claes, Hao Li, Emmanuel Audenaert

*From the Department of Orthopaedic Surgery and Traumatology, Ghent University Hospital, Ghent, Belgium*

**Aims : To apply cutting edge geometry processing techniques and statistical shape modelling to perform a quali-tative and quantitive evaluation of femoral deformity in developmental hip dysplasia and to describe its relation to the amount of acetabular coverage in full 3D.**

**An observational case-control study consisting of 40 right dysplastic cases compared to 43 normal hips, was designed. All subjects were Asian females with an average age of 53.9 years. The right femurs were scanned using computed tomography, followed by 3D reconstruction for statistical shape modelling. Inter-shape correspondences of the femoral shape were used to portray changes in femoral morphology to the amount of acetabular coverage. Partial least-squares regression was applied to establish a direct connection between acetabular coverage and the geometry of the femoral shape.**

**Acetabular coverage accounted for 7.1% of variation in the overal femur shape ($p<0.05$). Significant changes in femoral morphology ($p<0.05$) were observed with decreasing acetabular coverage. The regression model demonstrated progressive shortening of the femur neck, as well as increasing flattening of the femur head. Further, analysis of curvature and normal displacement demonstrated significant ($p<0.05$) flattening of the femur head especially in the area of the head-neck junction with increasing severity of acetabular dysplasia.**

**Anatomic abnormalities inherent to the dysplastic hip are limited to the very proximal part of the femur and significantly increase when the acetabular coverage decreases. Flattening of the femur head is most pronounced at the peripheral part of the head, in specific the femoral head-neck region.**

**Keywords :** Hip ; developmental dysplasia ; osteo-arthritis ; morphology.

## INTRODUCTION

Dysplasia of the hip is the most common cause for secondary osteoarthritis (OA), with the highest incidence in Asian populations making up to 88% of all OA cases in this area of the world

- Peter Mahieu[1].
- Takehito Hananouchi[2].
- Nobuyuki Watanabe[3].
- Peter Claes[4].
- Hao Li[5].
- Emmanuel Audenaert[1].

[1]*Department of Orthopaedic Surgery and Traumatology, Ghent University Hospital, Belgium.*

[2]*Department of Mechanical Engineering, Faculty of Engineering, Osaka Sangyo University, Japan.*

[3]*Department of Orthopaedic Surgery, Tosei General Hospital, Setoshi, Japan.*

[4]*Medical Image Computing, ESAT/PSI, Department of Electrical Engineering, University of Leuven, Belgium.*

[5]*Department of Computer Science, University of Southern California, USA.*

Correspondence : Audenaert Emmanuel, Department of Orthopaedic Surgery and Traumatology, Ghent University Hospital, De Pintelaan 185, B-9000 Ghent, Belgium, Tel. +32 93325699

E-mail : emmanuel.audenaert@ugent.be



*Emmanuel Audenaert was supported by the Flemish Research Foundation (FWO).*

*(20)*. Periacetabular osteotomy is the preferred non-prosthetic treatment after skeletal maturity and aims to restore normal coverage of the femur head. Such treatment, however, implies a well developed and spherical femur head . Several authors have observed substantial shape abnormalities of the femoral head with decreasing degrees of acetabular coverage and have warned for suboptimal joint articulation and secondary impingement compromising long-term outcome of periacetabular osteotomy for the treatment of developmental dysplasia of the hip (DDH) *(10,25)*. In the alternative case where joint replacement is considered, the procedure is technically challenging. Furthermore, results obtained from conventional femoral stem designs have been reported inferior with an increased incidence of loosening and dislocation in the long term *(6,12)*.

Various methods have been proposed to quantify and measure the complex femoral morphology in DDH *(4,19)*. Such tools are critical for clinical decision making and surgical planning. These reports are usually either qualitative or based on a limited number of simple measurements such as distances, distance ratios, angles, and other geometric approximations. With recent advances in computer graphics and vision, data-driven techniques allow us to explore a more grounded description of geometric shapes using large samples of input data *(11)*. With statistical shape models (SSM), it is possible to accurately describe the anatomy and its variation for any population using conventional multivariate statistics from sets of homologous dense landmarks captured by complete geometric shapes of the subject. Unlike existing approaches, these techniques provide accurate parameterizations of an individual's morphology and a consistent way of describing the anatomical distribution of an entire population. Moreover, these models are useful in improving the diagnosis, classification and treatment of specific medical conditions.

To date, the number of studies *(15,22)* on femoral morphology in DDH is limited. Furthermore, the relation between acetabular coverage and the degree of femoral dysplasia has not yet been studied with respect to the full 3D complexity of femoral anatomy. The aim of the present study is therefore to apply cutting edge geometry processing techniques and statistical shape modelling to perform a qualitative and quantitive evaluation of shape abnormalities of the femur in DDH and describe its relation to the amount of acetabular coverage in full 3D. It was hypothesized, in line with the observed differences reported in the current literature, that there would be significant differences in the morphology of the femur between the dysplastic cases compared to the controls.

## MATERIAL AND METHODS

The study was designed as an observational case-control study with a combined total of 83 Asian female subjects. All subjects were recruited at Osaka University Hospital and Tosei General Hospital in Japan during a two year period from the 1st of January 2012 till 31st of August 2013. The study was approved and performed according to the local ethical review board regulations.

For the dysplastic group, 40 cases of right-sided DDH were included in the study (average age 55.2 years; range 25-79 years). Diagnosis was based on a clinical and radiographical presentation of DDH. CT scans of the right hip and femur were obtained in the process of preoperative evaluation. None of these patients had a preceding osteotomy or hip arthroscopy for treatment or correction of their hip disease. For the control group, 43 unmatched right femurs were included with a normal anatomy of the proximal femur (average age 52.6 years; range 19-82 years). Controls were retrospectively recruited from an imaging database of angio-CT images, all obtained for investigation of non-orthopaedic conditions. The exclusion criteria for the control group were: (1) radiographical evidence of hip abnormalities, (2) clinical history of hip pain or (3) previous hip surgery.

All patients were scanned on a multidetector CT (Aquilion PRIME, Toshiba Medical Systems Corp., Tochigi, Japan). Slice thickness was 1 mm. The CT images were loaded in a 3D image processing software system (Mimics® 14.12, Materialise, Haasrode, Belgium) to create smooth 3D surface models of the right femur bones.

Dense anatomical point correspondences were obtained using a state-of-the-art non-rigid registration algorithm of Li *et al.* (17) where an isotropic template mesh (21096 vertices) of a femur is automatically aligned to any given sample scan *(5)*. Once we have aligned the intial 3D mesh with every sample, we calculate the average femur shape and re-compute the correspondences between the average shape and the input scans. The non-rigid alignment approach is based on an iterative closest point algorithm, that iterates between finding the closest points and optimizing for a deformation that maximizes local rigidity and smoothness. The optimization is formulated as an energy minimization where rigidity and smoothness are achieved by enforcing affine transformations of a vertex to be as close as possible to a rigid motion and neighbouring vertices to be similar. The non-linear optimization also uses a point-to-plane fitting term to promote correspondence optimization during the deformation. To effectively avoid local minima, the algorithm starts with a high-stiffness parameter for the rigidity constraint and relaxes the local rigidity parameter whenever convergence is detected. We use the same optimization parameters as described in the work of Li *et al. (17)*, and perform 250 iterations for each CT scan. The algorithm requires no manual input and establishes dense correspondences between all input scans robustly by smoothly warping the template model to arbitrary CT scans while avoiding unnatural distortions (deviations from local rigidity) during the fitting procedure (Fig. 1).

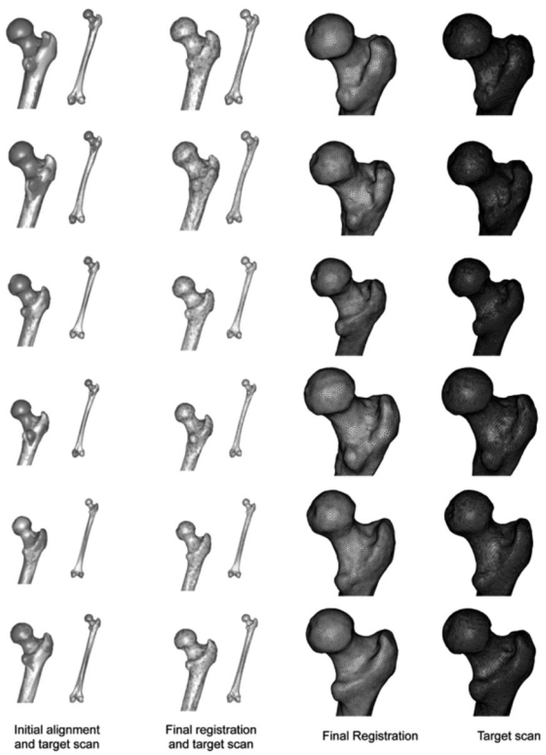


***Fig. 1.*** — Illustration of the registration process of the surface meshes: Each row represents a different femur example. The target scan is the mesh created from the original 3D reconstructed femoral bone. First an initial alignment of the template isotropic mesh is performed with a preliminary rigid registration algorithm (1st column). Second, elastic registration is applied to transform an isotropic template mesh of 21096 vertices to closely match the target scan (2nd column). The final result in column 3 shows the overlay of the registered mesh onto the original target scan of the femur bone (column 4).

Following robust least squares rigid alignment (Procrustes transformation) of these homologous series of dense landmarks, the variance of morphological differences within the femur was established by means of principal component analysis (PCA). It is important to note that the current sampling set contains femur models characterised by local dysmorphologies (e.g. a pronounced trochlear bump), which can lead to alignment errors. These abnormalities are typically spatially localized and do not extend over the whole region of interest. To account for general disturbance during alignment of the data sets by these local abnormalities, – the so-called Pinocchio-effect – iterative exclusion of outliers with a threshold value of 0.05 was performed to obtain a robust alignment prior to the PCA computation *(8)*.

In all cases radiological measurements were automated following the anatomical registration procedures, using custom-written software application in Matlab (MathWorks, Natick, Massachusetts). As such any observer related variation in landmarking could be excluded. The following parameters were measured: caput-collum-diaphyseal (CCD) angle *(27)*, femoral anteversion *(23)*, femoral offset *(6)*, lateral center edge (CE) angle of Wiberg *(29)* and the head sphericity index *(25)*. An overview of the applied definitions of these parameters is provided in table 1. Acetabular coverage was expressed by

Table 1. — Imaging parameters used to describe variation in hip joint morphology among subjects. CCD angle: caput-collum-diaphyseal angle.

| Parameter | Definition | Author | Normal Value |
|---|---|---|---|
| **CCD angle** | Angle formed by the axis of the femoral neck and the proximal femoral diaphyseal axis | Tönnis and Heinecke (1999)[27] | More than 125°; less than 135° |
| **Femoral anteversion** | Angle between the axis through the femoral neck with reference to the tangent to the posterior border of the femoral condyles | Rippstein (1955)[23] | Relative retroversion <15° Absolute retroversion <0° |
| **Femoral offset** | Length corrected distance from the center of rotation of the femoral head to a line bisecting the long axis of the femur | Charnley (1973)[6] | 2.5-5.5 cm |
| **Lateral center edge angle** | Angle formed by a line parallel to the longitudinal pelvic axis and by the line connecting the center of the femoral head with the lateral edge of the acetabulum | Wiberg (1939)[29] | More than 25°; less than 40° |
| **Head Sphericity Index** | Ratio of the length of the semi-minor axis and the length of the semi-major axis of the ellipsoid fitted to the surface of the femur head. The closer this index is to 1, the more the femur head resembles a sphere. | Stepacher et al. (2008)[25] | Larger than 0.9 |

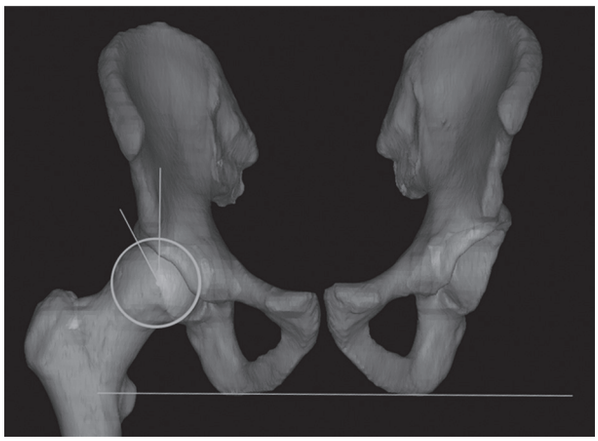

***Fig. 2.*** — Acetabular coverage was evaluated by means of the lateral center edge angle measured on the transparent 3-dimensional pelvis model

means of the lateral center edge angle using the transparent 3-dimensional pelvis model. (Fig. 2)

To investigate the differences in femoral bone geometry between the DDH and control femurs the mean shape of both femur sets was calculated and compared following rigid alignment of the two mean shapes. Point-wise surface variation between the average DDH and control model was expressed by visualizing the magnitude and direction of vectors between the corresponding surface vertices. Differences between the two correspondent data sets were statistically determined by means of the student's t-test at an alpha level for significance of 0.05.

To describe shape variations within the study population, principal component analysis (PCA) is applied on the corresponding vertices of the 40 DDH and 43 control surface meshes *(28)*. PCA consists of computing the statistically independent eigenvectors and eigenvalues of the data set. The eigenvectors (principal components) show global shape variations, called 'modes of variation' in a SSM. The associated eigenvalues indicate the amount of shape variance explained by that specific mode of shape variation. The eigenvectors are ordered according to their explained variance; eigenvectors with highest variance are placed first and those with low variance are placed last.

To evaluate how well the model describes the overall populations a complete "leave one out" assessment was performed. To do so, a SSM was constructed, iteratively leaving one selected test bone out. Subsequently, the SSM was fitted to the excluded bone and the goodness of fit of the SSM to describe a bone not included in the SSM was evaluated. As error measure the RMS distance was computed between the fitted sample and the corresponding vertices of the excluded bone. This procedure was repeated for all bones in the DDH

group and the control group. The RMS errors for all femur models are an indication of the quality of the SSM.

Femoral coverage by the acetabulum was quantified by means of the corresponding CE angles. A regression model was then developed linking CE angles to the shape modes of all the femurs (43 controls and 40 DDH cases) in the training set of the model. Considering the large number of available predictors, partial least squares regression (PLS regression) was chosen as the preferred methodology over the well known regular multiple regression technique. Subsequently, the linear relationship between acetabular coverage and the amount of femoral head deformity was established. Sphericity and overall shape of the proximal femur were qualitatively and quantitatively evaluated in relation to the average control femur. Furthermore, local shape curvatures were computed and tested for significance in change in relation to the CE angle and displayed. The signed mean curvature in each anatomical point-correspondence was used where a negative and positive sign indicate a concave and convex local shape, respectively. A curvature of zero indicates a locally flat shape. Positive (H1+) and negative (H1-) one-sided tests and two-sided tests (H2) are performed using 10,000 permutations following the framework described by Claes P *et al.* *(7)*. The level of significance was set at a p-value of 0.05. The effect-size or strength of the relationship between the lateral CE angle was reported as the variance in the training set explained by the PLSR model *(2)*. Statistical significance of the effect-size is tested under permutation (1,000 permutations) for multivariate regressions *(2)*. In essence, the overall effect size is the amount of femural variation coded in all quasi-landmarks that is explained by the lateral CE angle.


***Fig. 3.*** — Point-wise differences (mm) in average femur surface geometry between the control and the DDH group projected on the surface geometry of the dysplastic normal femur. The morphological diffences are mainly limited to the femoral neck and head.

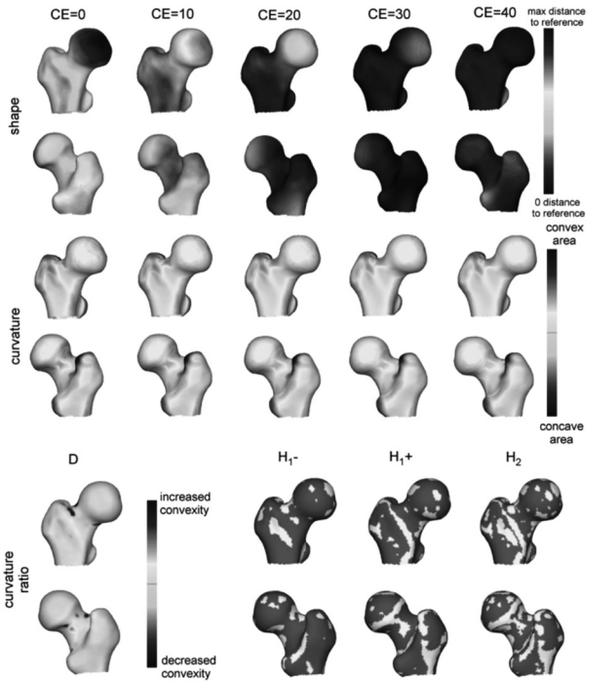


***Fig. 4.*** — A. Shape changes of the femoral head with increasing acetabular coverage (CE). Colours indicate the pointwise distance to the average control. The first row shows the front view; the second row the back view. Surface curvature changes with increasing CE is presented in the third (front view) and fourth (back view). Red or blue colours indicate respectively a convex or a concave area. Pointwise ratios (D) between the surface curvatures at CE=40 and those at CE=0, and the results of the permutation tests for negative (H1-) and positive (H1+) one-sided tests, and for two-sided test (H2) are presented in the last two rows. For the curvature ratios, a red or blue area indicates respectively a region of increased or decreased convexity. For the permutation tests, yellow indicates a significant result. A yellow region in the H1- plot indicates an area of significant decreased convexity. A yellow region in the H1+ plot indicates an area of significant increased convexity.

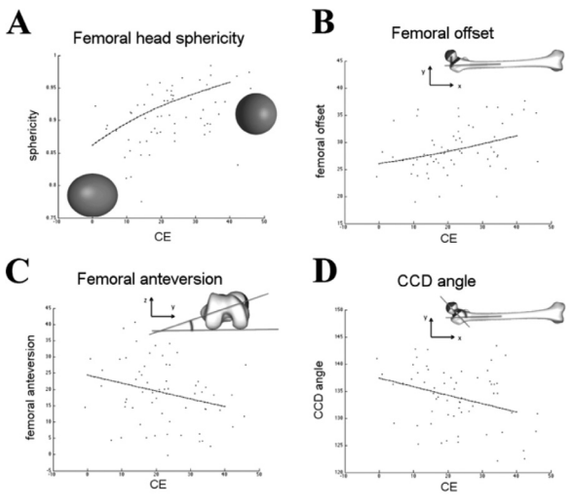


***Fig. 5.*** — A: Relation between acetabular coverage and femoral head sphericity as predicted by the regression model (line plot) and as observed in the training set (scatter plot). B: Relation between acetabular coverage and femoral head offset. C: Relation between acetabular coverage and femoral anteversion. D: Relation between acetabular coverage and the femoral CCD angle.

## RESULTS

The quality evaluation of the SSM, using all principal components, showed an average root mean square (RMS) error of 0.87 mm (SD +/- 15 mm) for the control group and 0.74 mm for the DDH femurs (SD +/- 0.18 mm). The average DDH femur was significantly smaller and anteverted at the level of the femur head and neck compared to the average control femur. Further, the average DDH femur showed loss of sphericity in addition to an increased valgus. Interestingly, all of these differences were exclusively present in the proximal part of the femur, commencing only at the level of the femur neck. An overview of demographic and radiographic findings and their distribution in the respective population is provided in table 2. Point-wise surface differences between the average DDH and control model are demonstrated by a colour plot on the surface model of the average control in figure 3.

Qualitative evaluation of the PLSR model demonstrated that acetabular coverage accounted for 7.1% of variation in the overal femur shape ($p < 0.05$). Macroscopic analysis of shape evolution within the PLSR model with decreasing acetabular coverage of the femur head demonstrated progressive shortening of the femur neck, as well as increasing flattening of the femur head. A detailed overview of the PLSR model is provided in figure 4. Analysis of curvature and normal displacement demonstrated significant ($p<0.05$) flattening of the femur head in the area of the head-neck junction. Only scattered changes in curvature were observed in the central part of the femur head.

A detailed analysis of changes in anatomical features within the PLSR model demonstrated a non-linear increase in CCD angle and femoral anteversion in dysplastic hips compared to controls. The femoral offset and head sphericity, on the other

Table 2: Comparison of demographic and radiographic data of the dysplasia ( DDH ) group and the control group.

| | DDH (N=40) | Controls (N=43) | p Value |
|---|---|---|---|
| **Age (years)** | 55.2 (SD 15.6) | 52.6 (SD 14.5) | 0.431 |
| **Gender (% female)** | 100 | 100 | 1.000 |
| **Origin (% Asia)** | 100 | 100 | 1.000 |
| **Femur length (cm)** | 38.3 (SD 1.8) | 40.6 (SD 2.4) | <0.001 |
| **Lateral center-edge angle (degrees)** | 15.6 (SD 6.6) | 34.4 (SD 5.8) | <0.001 |
| **Femoral anteversion (degrees)** | 21.0 (SD 9.9) | 14.2 (SD 9.3) | 0.002 |
| **Caput-collum diaphyseal angle (degrees)** | 134.7 (SD 5.2) | 132.1 (SD 5.0) | 0.021 |
| **Femoral offset (cm)** | 2.8 (SD 0.4) | 3.2 (SD 0.4) | <0.001 |
| **Femoral head sphericity** | 0.89 (SD 0.04) | 0.94 (SD 0.03) | <0.001 |

hand, were found to be non-linearly decreased in dysplastic hips (figure 5).

## DISCUSSION

Femoral deformities associated with acetabular dysplasia have been well documented in the literature *(26)*. The most common deformations include femoral anteversion, an aspheric femoral head, and reduced femoral head-neck offset. Our findings are in line with these reports. Nevertheless, there has been limited comprehensive information regarding these deformations relative to the general morphology of the femur as to the severity of the disease. In the present study we were able to demonstrate that the deformations are almost exclusively present in the femur head neck region and correlate importantly with the amount of coverage as quantified by the CE angle. Further, it appears that sphericity is largely comprimised for CE angles from 20 degrees on. For these cases, joint congruency might be insufficient to provide good long term perspectives with peri-acetabular osteotomy .

The finding of normal contours of the femur shaft in the present study is not entirely surprising but further verified. Back in 1996, Robertson and colleagues *(24)* developed a quantitative 3 dimensional model of deformations of the femur in developmental dysplasia of the hip. In this particular work, a SSM "avant la lettre", they found no statistical correlation between the femur shaft morphology and the severity of the disease. Hence, it appears at first sight that conventional prosthetic designs might suffice for these patients. Clearly this is not in line with the available reports on the technical difficulties encountered in this patient group, as well as the notable higher rate of cortical fractures reported in THA for patients with dysplastic hips *(14)*. However, this can be partially explained, by the tendency of dysplasia patients to be smaller in stature and quite typically of female gender *(3)*, a finding that was further confirmed in the present study. Therefore, sizing using conventional products might be problematic and partially explain the encountered fracture risks.

Many previous studies have attempted to describe femoral morphology in DDH. The majority of these reports are based on conventional radiography, and only a few have used 2D reconstructions of volumetric imaging. Nevertheless, there have been a few detailed scientific studies that have evaluated the deformity of the femur taking into account its entire morphology *(22,24)*. Noble and colleagues used 3D, surface-splined models to analyze femoral deformity between DDH versus controls. In contrast to Robertson and the present study, they found significant differences in shaft morphology between the two groups. However, this finding could be explained by the lack of dense anatomical correspondence between their models to drive a robust alignment procedure before the actual anatomical analysis was performed. Technical reports have undeniably demonstrated that important interpretation errors can occur for incomplete and inaccurate measurements, particularly for regional abnormalities *(8,9)*.

An additional advantage of the applied techniques in the present study is that it enables a quantified measurement of the severity of the disease by analyzing the magnitude of geometric features. Particularly interesting for clinical studies is the evolution in sphericity of the femur head as described by our curvature analysis. The occurrence of labrum lesions is well known in the literature. Some attribute this to mechanical overloading, others to instability of the joint. In the present study it appeared that curvature did not significantly change in the central part of the femur head – i.e. the part most in contact with the acetabulum – as compared the peripheral border. This results in a third mechanism for labrum damage: mechanical impingement by a aspherical femoral head neck junction. Therefore, even a dysplastic hip has the potential to develop symptoms similar to femoroacetabular impingement. In addition, this finding underlines the increasing risk for secondary impingement following osteotomy in the severe dysplastic hip. Furthermore, this asphericity might contribute to dynamic hip instability and labrum damage as previously suggested by Akiyama *et al. (1)* and Maeyama *et al. (18)*. Clearly, further explorations in this direction are necessary to address these findings.

Although the present study shows an important correlation between the deformity of the femur head and the amount of acetabular coverage as expressed by the CE angle, such correlation nearly describes the co-occurrence of anatomical features but fails to draw any conclusions related to causality: does femoral deformity depend on the amount of acetabular coverage or vice versa. Most likely, there is a mutually dependent relationship in the development of a congruent hip *(16)*. The morphological development of the femur head and the acetabulum depends on the interaction of the two structures and any abnormality in one will affect the development of the other *(13)*.

A second limitation of the present analysis involves the selected study population. Because DDH is relatively uncommon in the American and European population as compared to the Asian population, we have focussed on a female Asian study population. However, it is well know that shape of the human femur greatly varies with gender, age, stature and ethnic background of each individual. The results might therefore not directly be generalized to all patients with hip dysplasia *(21)*. Nevertheless we expected that the general principles as described in the present work will largely apply to European and American patients as well. Obviously such assumptions need further investigation in the future.

To conclude, the present study demonstrates that the anatomic abnormalities inherent to the dysplastic hip are limited to the very proximal part of the femur and significantly increase with decreasing acetabular coverage, notable decreasing offset, increasing anteversion, valgus and flattening of the femur head. Further it appears that flattening of the femur head is most pronounced at the peripheral part of the head, in specific the femoral head-neck region.

## REFERENCES


1. **Akiyama K, Sakai T, Koyanagi J, Yoshikawa H, Sugamoto K**. Evaluation of translation in the normal and dysplastic hip using three-dimensional magnetic resonance imaging and voxel-based registration. *Osteoarthritis and Cartilage.* 2011 ;19 : 700-10.
2. **Anderson MJ**. Permutation tests for univariate or multivariate analysis of variance and regression. *Canadian Journal of Fisheries and Aquatic Sciences.* 2001 ; 58 : 626-39.
3. **Argenson JN, Flecher X, Parratte S, Aubaniac JM**. Anatomy of the dysplastic hip and consequences for total hip arthroplasty. *Clin Orthop Relat Res*. 2007 ; 465 : 40-5.
4. **Audenaert EA, Baelde N, Huysse W, Vigneron L, Pattyn C.** Development of a three-dimensional detection method of cam deformities in femoroacetabular impingement. *Skeletal Radiology*. 2010 ; 40 : 921-7.
5. **Botsch M, Kobbelt L.** A remeshing approach to multi-resolution modeling. Proceedings of the 2004 Eurographics/ ACM SIGGRAPH symposium on Geometry processing - SGP '04; 2004 Jul: Association for Computing Machinery (ACM); 2004.
6. **Charnley J, Feagin JA**. Low-Friction Arthroplasty in Congenital Subluxation of the Hip. *Clin Orthop Rel Res.* 1973 ; 91 : 98-113.
7. **Claes P, Daniels K, Vandermeulen D, Suetens P, Shriver MD.** A PLS Regression Framework for Spatially-dense Geometric Morphometrics to Analyze Effects on Shape and Shape Characteristics: Applied to the Study of Genomic Ancestry and Sex on Facial Morphology. *Biological Shape Analysis*; 2015 May: World Scientific Pub Co Pte Lt; 2015.
8. **Claes P, Daniels K, Walters M, Clement J, Vandermeulen D, Suetens P.** Dysmorphometrics: the modelling of morphological abnormalities. *Theor Biol Med Model.* 2012 ;9 : 5.
9. **Claes P, Walters M, Clement J.** Improved facial outcome assessment using a 3D anthropometric mask. *Int J Oral Maxillofacial Surg.* 2012 ; 41 : 324-30.
10. **Clohisy JC, Nunley RM, Carlisle JC, Schoenecker PL**. Incidence and Characteristics of Femoral Deformities in the Dysplastic Hip. *Clin Orthop Relat Res*. 2008 ; 467 : 128-34.
11. **Cootes TF, Taylor CJ.** Anatomical statistical models and their role in feature extraction. *BJR.* 2004 ; 77 : S133-S9.
12. **Crowe JF, Mani VJ, Ranawat CS.** Total hip replacement in congenital dislocation and dysplasia of the hip. *J bone joint surg (Am)* 1979 ; 61 : 15-23.
13. **Grzegorzewski A, Synder M, Kozlowski P, Szymczak W, Bowen RJ.** The Role of the Acetabulum in Perthes Disease. *J Pediatric Orthop* 2006 ; 26 : 316-21.
14. **Haddad FS, Masri BA, Garbuz DS, Duncan CP.** The Treatment of the Infected Hip Replacement. *Clin Orthop Relat Res* 1999 ; 369 : 144-56.
15. **Khang G, Choi K, Kim C-S, Yang JS, Bae T-S.** A Study of Korean Femoral Geometry. *Clin Orthop Relat Res* 2003 ; 406 : 116-22.
16. **Lee MC, Eberson CP.** Growth and Development of the Child's Hip. Orthopedic Clinics of North America. 2006 ; 37 : 119-32.
17. **Li H, Adams B, Guibas LJ, Pauly M.** Robust single-view geometry and motion reconstruction. ACM SIGGRAPH Asia 2009 papers on - SIGGRAPH Asia '09 ; 2009 Dec : Association for Computing Machinery (ACM) ; 2009.
18. **Maeyama A.** Evaluation of Dynamic Instability of the Dysplastic Hip with Use of Triaxial Accelerometry. The Journal of Bone and Joint Surgery (American). 2008 ; 90 : 85.

19. **Masjedi M, Harris SJ, Davda K, Cobb JP**. Mathematical representation of the normal proximal human femur : Application in planning of cam hip surgery. Proceedings of the Institution of Mechanical Engineers, Part H : Journal of Engineering in Medicine. 2012 ; 227 : 421-7.
20. **Nakamura S, Ninomiya S, Nakamura T.** Primary Osteoarthritis of the Hip Joint in Japan. *Clin Orthop Relat Res* 1989 : 190-6.
21. **Noble PC, Box GG, Kamaric E, Fink MJ, Alexander JW, Tullos HS.** The Effect of Aging on the Shape of the Proximal Femur. *Clin Orthop Relat Res* 1995 : 31-44.
22. **Noble PC, Kamaric E, Sugano N, Matsubara M, Harada Y, Ohzono K, et al.** Three-dimensional shape of the dysplastic femur : implications for THR. *Clin Orthop Relat Res* 2003 : 27-40.
23. **Rippstein J.** [Determination of the antetorsion of the femur neck by means of two x-ray pictures]. Zeitschrift fur Orthopadie und ihre Grenzgebiete. 1955 ; 86 : 345-60.
24. **Robertson DD, Essinger JR, Imura S, Kuroki Y, Sakamaki T, Shimizu T, et al.** Femoral Deformity in Adults With Developmental Hip Dysplasia. *Clin Orthop Relat Res* 1996 ; 327 : 196-206.
25. **Steppacher SD, Tannast M, Werlen S, Siebenrock KA**. Femoral Morphology Differs Between Deficient and Excessive Acetabular Coverage. *Clin Orthop Relat Res*. 2008 ; 466 : 782-90.
26. **Sugano N, Noble PC, Kamaric E, Salama JK, Ochi T, Tullos HS.** The morphology of the femur in developmental dysplasia of the hip. *J bone joint surg (Am)* 1998 ; 80 : 711-9.
27. **Tonnis D, Heinecke A.** Acetabular and femoral anteversion : relationship with osteoarthritis of the hip. *J bone joint surg (Am)*. 1999 ; 81 : 1747-70.
28. **Webb AR.** Statistical Pattern Recognition :Wiley-Blackwell ; 2002 2002 Jul.
29. **Wiberg G.** Studies on dysplastic acetabula and congenital subluxation of the hip joint : with special reference to the complication of osteoarthritis. *Acta Chir Scand*. 1939 ; 83 : 53-68.